Journal of Molecular Liquids 271 (2018) 166–174

Contents lists available at ScienceDirect

Journal of Molecular Liquids

journal homepage: www.elsevier.com/locate/molliq

Effect of polystyrene length for the extraction of Gd^{3+} and UO_2^{2+} ions using dicyclohexano crown ether (DCH18C6) with octanol and nitrobenzene: A molecular dynamics study

Praveenkumar Sappidi, Showkat Hassan Mir, Jayant K. Singh *

Department of Chemical Engineering, Indian Institute of Technology (IIT) Kanpur, Kanpur 208016, India

ARTICLE INFO

Article history:
Received 13 June 2018
Received in revised form 20 August 2018
Accepted 24 August 2018
Available online 29 August 2018

Keywords:
Dicyclohexano crown ether (DCHCE)
Binding free-energy
Transfer free-energy
Partition coefficient
MD simulation
Gadolinium
Uranyl

ABSTRACT

The role of polystyrene (PS) grafting to the dicyclohexano crown ether (DCHCE) in extracting the Gd^{3+} and UO_2^{2+} is evaluated for the first time using atomistic molecular dynamics (MD) simulations. The thermodynamic free-energy (ΔG_{Bind}) is calculated to understand the binding of Gadolinium (Gd^{3+}) and Uranyl (UO_2^{2+}) to the DCHCE in nitrobenzene (NB) and octanol (OCT) solvents. The results show that the binding free-energy is favorable for Gd^{3+} and UO_2^{2+} in NB, and unfavorable in OCT. In NB, the ΔG_{Bind} of Gd^{3+} and UO_2^{2+} increases by 2.3% and 3.1% respectively with an increase in the PS length from 0 to 3. On the contrary, in OCT, the ΔG_{Bind} of Gd^{3+} and UO_2^{2+} decreases by 2.4% and 3.4% with an increase in PS length of the grafted DCHCE. The transfer free-energy ($\Delta G_{Transfer}$) for both the ions viz., Gd^{3+} and UO_2^{2+}, from the aqueous phase to an organic phase is also analyzed using NB and OCT as extractants. The $\Delta G_{Transfer}$ for both ions shows encouraging extraction ability in NB while the extraction ability decreases using OCT as an extractant. The partition coefficient (log P) values show an increase with an increase in PS grafting length on the DCHCE using NB as an extractant, while an opposite behavior is observed in OCT. In particular, with increase in the PS length, for Gd^{3+} and UO_2^{2+}, log P values in NB increase by 13% and 9.6% respectively; whereas log P values decrease by 27% and 10% in OCT. In the presence of acidic medium (3 M HNO_3 solution) the $\Delta G_{Transfer}$ values for both Gd^{3+} and UO_2^{2+} show ~6% and 9% increase with NB and OCT, respectively. The structural and thermodynamic solvation properties are in accordance with the observed ΔG_{Bind}, $\Delta G_{Transfer}$, and log P.

1. Introduction

Extraction of lanthanides and actinides from the high-level nuclear waste is a major problem in the nuclear industry due to the difficulty in extracting the toxic gadolinium (Gd^{3+}) and uranyl (UO_2^{2+}) from the high nuclear waste. The macrocyclic polyethers such as crown ethers have been effectively used for the recovery or extraction of lanthanides and actinides in the form of stable metal ion – crown ether complexes [1–7]. The selection of suitable ligand from numerous possibilities for the recovery of specific metal ion depends on the cavity and metal ion diameters have been recognized by various molecular simulation studies and experiments [7–12]. Both experiments and molecular simulations have demonstrated that dibenzo-crown-ether (DB18C6 or DBCE) and dicyclohexano crown ether (DCH18C6 or DCHCE) are suitable ligands for the extraction of Gd^{3+} and UO_2^{2+}. [1,3,13–16].

The organic solvent such as alcohols as an extractant has been shown to play a major role in enhancing the extracting capabilities of ligands through the formation of stable ligand metal-ion complexes [4,6,7,11,14,15,and]. It is shown that the presence of organic solvent in the solution containing crown ether and metal ions further improves the binding of metal ions with the crown ethers [11–15]. The free-metal ions bind on to the oxygen's of crown-ethers via significant electrostatic interaction leading to tight binding with crown ethers [15,16]. For example, the presence of organic solvent like nitromethane and acetonitrile (ACN) enhance the significant extraction of metal ions such as UO_2^{2+}, Pb^{2+}, Ba^{2+} and Cd^{2+} with DCHCE as observed by the conductometric study [7]. A conductometric study by Rounaghi et al. [4] demonstrated that Gd^{3+} show improved complexation with DCHCE as compared to mono-cations such as NH_4^+ and Ag^+ in the mixture of an organic solvent containing tetrahydrofuran (THF) and ACN. The experimental study by Boda. et al. [14,15] have shown that nitrobenzene (NB) and octanol (OCT) act as good extractants for separation of Gd^{3+} and strontium Sr^{2+} from the radioactive waste in the form of stable metal ion crown-ether complexes. Due to the above role of solvent, liquid-liquid extraction is highly accepted method for the separation of heavy metal ions from the high-level radioactive waste.

In a series of recent works, it is revealed that polymer grafted crown ether augments the binding of the metal ion with crown ether [15–18]. An experimental study by Ye et al. [3] has shown that polysiloxane

* Corresponding author at: Dept. of Chemical Engineering, IIT Kanpur, UP 208016, India.
E-mail address: jayantks@iitk.ac.in (J.K. Singh).

https://doi.org/10.1016/j.molliq.2018.08.133
0167-7322/

based DCHCE exhibited enhanced extraction capacity for Sr^{2+} using OCT. Sinta et al. [17] have developed polystyrene (PS) based ligand for the effective binding of sodium (Na^+) and potassium (K^+). A combined experimental and theoretical study of Boda et al. [15] showed that PS grafted crown ethers such as DB18C6 and DCH18C6 increases the binding of Gd^{3+}. A recent MD simulation study [16] demonstrated that increasing the PS grafting length on the DBCE show significant extractions of Gd^{3+} and UO_2^{2+} from an aqueous solution, and fivefold increase in the partition coefficient values. Furthermore, UV/Vis spectroscopy showed that polymer-supported crown ether exhibits thermodynamically stronger complexation for the metal ion [18].

However, despite the available experimental and simulation results not much is known about the complexation of the metal ions such as Gd^{3+} and UO_2^{2+} with polymer supported DCHCE. There are several questions yet to be answered such as: a) binding affinity of Gd^{3+} and UO_2^{2+} with bare and polymer supported DCHCE; b) the role of polystyrene grafting in extracting these metal ions using liquid-liquid extraction as organic solvents as an extractant; c) the separation efficiency of the polymer grafted DCHCE using NB and OCT as extractants; d) and the thermodynamics of binding and transfer of the Gd^{3+} and UO_2^{2} ions from an aqueous phase to an organic phase. In this work, we have used molecular dynamics simulation to address the above questions, which would help in selecting suitable ligands and organic solvents for the effective extraction of heavy metal ions. Thus, the main objective of this study is to understand the effect of polystyrene grafting on DCHCE in enhancing the binding free-energy (ΔG_{Bind}) of Gd^{3+} and UO_2^{2+} in NB and OCT solvents.

2. Methodology and simulation details

We have considered four DCHCE for this study viz., (1) DCHCE-0PS (without polystyrene grafting), (1) DCHCE-1PS (one monomer of polystyrene grafting on the both sides of DCHCE), (3) DCHCE-2PS (two monomers of polystyrene grafting on the both sides of DCHCE) and (4) DCHCE-3PS (three monomers of polystyrene grafting on the both side of DCHCE). The input structures of these crown ethers are prepared in Materials studio [19]. Geometry optimization of these four structures was performed using density functional theory (DFT) using Gaussian09 [20]. All calculations were performed using B3LYP [21] hybrid functional and 6–31 g(d,p) basis set for C, H and O while LANL2DZ effective core potential applied to the heavier atoms. The same level of theory was employed for the charge calculations using ChelpG method [22]. In order to perform MD simulations, Gd^{3+} and UO_2^{2+} ions were placed in the cavity of DCHCE. Fig. 1 presents the DFT optimized structures of Gd^{3+}-DCHCE and UO_2^{2+}-DCHCE at various PS grafting lengths used in the MD simulations. Tables S1–S4 in the supplementary file list all the force-field parameters used in this work. All-atom OPLS force field [23] is used for DCHCE, NB and OCT solvents and Gd^{3+} and UO_2^{2+} ions. In the case of simulation where acidic medium is considered, the acidic

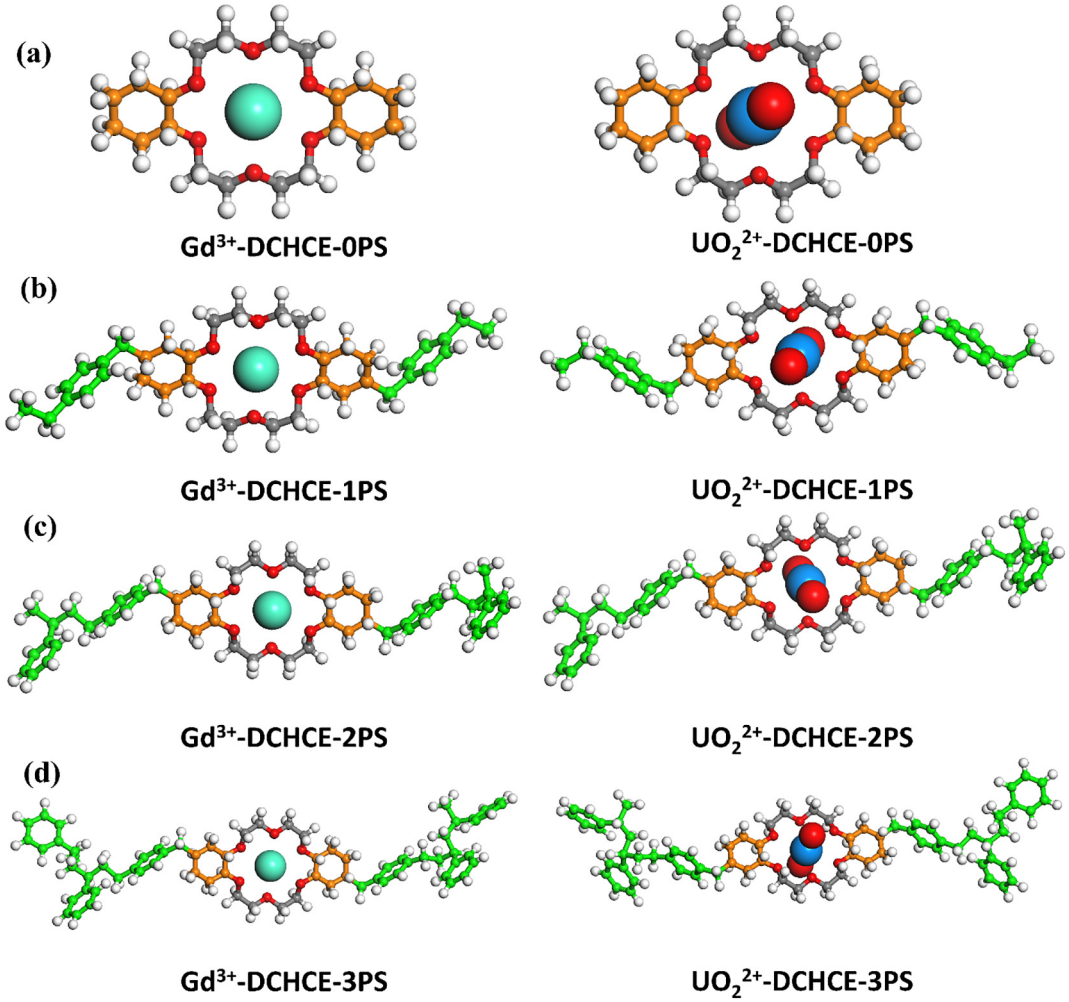

Fig. 1. Schematic representation of ion complexed crown ethers with (a) DCHCE, (b) DCHCE-1PS, (c) DCHCE-2PS and (d) DCHCE-3PS. Color Codes: Gray-carbon, white-hydrogen, red-oxygen, orange-benzene, green-polystyrene, cyan-gadolinium, and blue-uranium. (For interpretation of the references to color in this figure legend, the reader is referred to the web version of this article.)

medium (3 M) is maintained by explicitly considering the H_3O^+ and NO_3^- ions. The bonded and non-bonded interaction parameters are taken from our earlier work [16]. The electrostatic interactions were calculated using particle mesh Ewald (PME) [26] with a cut-off radius of 1 nm. The van der Waals interactions were calculated using Lennard-Jones 6–12 potential with a cut-off radius of 1.4 nm. All the bond lengths were constrained using LINCS method [27].

Temperature and pressure were kept constant at 300 K and 1 atm using Nosé–Hoover thermostat and Parrinello-Rahman barostat, respectively. The equation of motion was solved using leap-frog algorithm and 2 fs time step. The energy minimization was performed using the steepest decent method. Potential energy minimization and MD simulations were performed using Gromacs (version 4.5.5) [28].

The structural properties and density of NB and OCT were calculated using the same methodology as in our previous work [16]. First Gd^{3+} and UO_2^{2+} ion complexed DCHCE were placed in the equilibrated solvents of NB and OCT separately. NO_3^- counter-ions were added to the simulation system for the charge neutrality. We have first performed 100 ps NVT simulation followed by 100 ps NPT simulation. The production run was performed for 15 ns and data were collected for every 500 steps. The last 5 ns of the trajectory was used to evaluate average properties.

The binding free energy of the metal ion in the crown ether is evaluated by growing the metal in the cavity of crown ether in the presence of two organic solvents: NB and OCT. The two-stage thermodynamic integration (TI) method was used to calculate free energy difference of unbound state to the fully bound state. In the two-stage TI, we grow the electrostatic and van der Waals interactions separately. The detailed information about the two-stage thermodynamic integration procedure is clearly described in Ref [16]. Using the two-stage thermodynamic integration procedure the ΔG_{Bind} can be described as

$$\Delta G_{Bind} = \Delta G_{LJ} + \Delta G_C \tag{1}$$

This can be further expanded as

$$\Delta G_{Bind} = \int_{\lambda_{LJ}=0,\lambda_C=0}^{\lambda_{LJ}=1,\lambda_C=0} \left\langle \frac{\partial U(\lambda)}{\partial \lambda} \right\rangle_\lambda d\lambda + \int_{\lambda_{LJ}=1,\lambda_C=0}^{\lambda_{LJ}=1,\lambda_C=1} \left\langle \frac{\partial U(\lambda)}{\partial \lambda} \right\rangle_\lambda d\lambda \tag{2}$$

where λ_C and λ_{LJ} represent the coupling constants for coulomb and van der Waals interactions respectively. In the first stage (ΔG_{LJ}), we grow the metal from the initial state represented as $\lambda_{LJ} = 0$ and $\lambda_C = 0$ (i.e., there is no interaction) to a state with full LJ interaction but without Coulomb interaction i.e., $\lambda_{LJ} = 1$ and $\lambda_C = 0$. In the second stage (ΔG_C), we grow the ion from $\lambda_{LJ} = 1$ and $\lambda_C = 0$ to the state with full LJ and Coulombic interactions (i.e., $\lambda_{LJ} = 1$ and $\lambda_C = 1$). The schematic representation of entire thermodynamic cycle is presented in Fig. 2.

We calculate $\langle \partial U/\partial \lambda \rangle$ at different values of coupling parameters λ_{LJ} and λ_C. The λ_{LJ} and λ_C values were varied in steps of 0.05 in the range 0–1. We performed 42 simulations, in total, to calculate the value of binding free-energy. Transfer free energy ($\Delta G_{Transfer}$) is evaluated using the free-energy difference of metal ion from an aqueous phase to an organic phase using the relation:

$$\Delta G_{Tranfer} = \Delta G_{Bind} - \Delta G_{Hydration} \tag{3}$$

where the $\Delta G_{Hydration}$ is the hydration free-energy evaluated by performing the free energy simulation of free metal (Gd^{3+} and UO_2^{2+}) in water. This $\Delta G_{Transfer}$ is useful in estimating the efficiency of metal ion extraction from the aqueous solution to the organic solution in a liquid-liquid extraction process. This procedure is akin to that used by earlier workers [16,29,30,and]. The estimation partition coefficient log P was calculated directly using transfer free-energy.

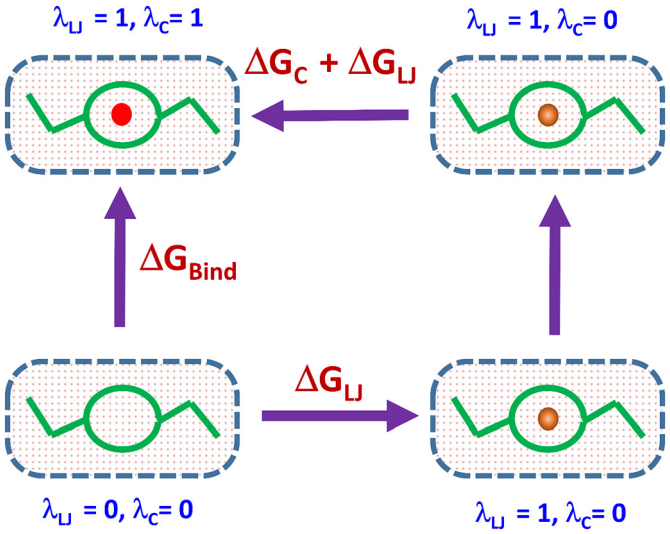

Fig. 2. Schematic representation of thermodynamic cycle for the estimation of binding free energy using thermodynamic integration.

The log P is directly proportional to the transfer free energy [29,30], as shown below:

$$\log P = \frac{\Delta G_{Bind} - \Delta G_{Hydration}}{2.303RT} \tag{4}$$

Here R is the molar Boltzmann constant and T is the temperature.

3. Results and discussion

3.1. Gd^{3+}-DCHCE and UO^{2+}-DCHCE solvation structure

The structural properties are investigated using the radial distribution functions (RDF). Fig. 3 presents the RDF between oxygen of crown ether (O_C) - oxygen of nitrobenzene (O_{NB}), O_C - oxygen of Octanol (O_{OCT}), O_C - nitrogen of nitrobenzene (N_{NB}) and O_C - hydrogen of Octanol (H_{OCT}) for the Gd^{3+}-DCHCE complex with an increase in the PS length. The first peak located at 0.45 nm for O_C-O_{NB}, 0.51 nm for O_C - N_{NB}, 0.28 nm for O_C - O_{OCT} and 0.18 nm for O_C - H_{OCT}. These results are in excellent agreement with the previous simulation studies [12,16]. The location of the peak does not significantly get influenced by the variation of PS length on the DCHCE. The corresponding coordination numbers (N_{cr}) do not show any significant change due to the PS grafting from 0PS to 3 PS, for the case of NB and OCT. The coordination numbers for the various atomistic pairs are summarized in Table 1.

Fig. 4 presents the RDF between O_C with solvent molecules for different PS lengths for the UO_2^{2+}-DCHCE complex. There are no significant structural changes observed when compared with the results of Gd^{3+}-DCHCE. To the best of our knowledge, no theoretical or simulation studies are available for the comparison of solvent and PS effect on the structural properties of Gd^{3+} -DCHCE and UO_2^{2+} -DCHCE. Nevertheless, structural properties of isolated Gd^{3+} and UO_2^{2+} ions in NB, OCT and water have already been compared in our recent work and are in good agreement with experiments and simulations [16].

3.2. Gd^{3+}-DCHCE and UO^{2+}-DCHCE solvation behavior

Fig. 5. presents the solvation enthalpy (ΔH_{solv}) of Gd^{3+}-DCHCE and UO_2^{2+}-DCHCE in two different solvents with increase in PS length. The thermodynamic solvation enthalpy is the difference between the total enthalpy of solution and enthalpy of solvent

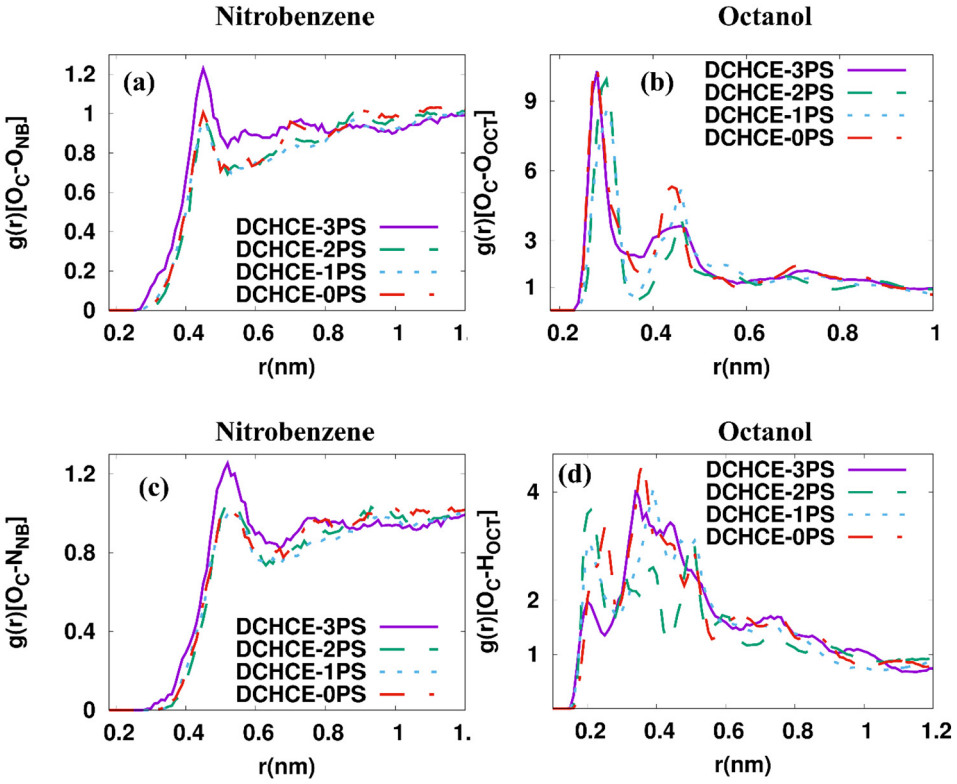

Fig. 3. RDF plot of (a) O_C–O_{NB}, (b) O_C–O_{OCT}, (c) O_C–N_{NB} and (d) O_C–H_{OCT} for Gd^{3+}-DCHCE.

and enthalpy of isolated solute in a vacuum, as shown in relation below:

$$\Delta H_{solv} = H_{solution} - (H_{solvent} + H_{isolated\ solute}). \quad (5)$$

where, $H_{solution}$ is the solution enthalpy of ion complexed DCHCE in a solvent, $H_{Solvent}$ is the enthalpy of the solvent and $H_{isolated\ solute}$ is the enthalpy of solute (i.e., DCHCE) in a vacuum.

The observed ΔH_{solv} of Gd^{3+}-DCHCE and UO_2^{2+}-DCHCE displays favorable values with an increase in PS length in the solvents NB, and OCT. Further, it is observed that the solvation becomes more favorable with an increase in PS length in OCT when compared to NB. It is apparent from the results that the electrostatic interaction plays a significant role in the ion complexed with DCHCE when compared to the van der Waals interaction.

The solubility of grafted ionophore (i.e., Gd^{3+}-DCHCE and UO_2^{2+}-DCHCE) in nitrobenzene and octanol is analyzed using the potential of mean force (PMF). The PMF is calculated using the relation given by w (r) = −kT ln (g(r)). The PMF curves of different atom pairs are shown in Figs. S1 and S2 of the supplementary data. It is seen that Gd^{3+}-DCHCE (Fig. S1) show lower PMF values in octanol as compared to nitrobenzene, which indicates that Gd^{3+}-DCHCE is more soluble in octanol. The PMF value of Gd^{3+}-DCHCE in presence of NB is −0.8 kJ/mol, which is not much affected by the increase in PS grafting length. However, PMF value in the presence of octanol increases from −5.8 kJ/mol to −5.1 kJ/mol with an increase in PS grafting length from 0PS to 3PS.

Similarly for UO_2^{2+}-DCHCE the PMF values (Fig. S2) does not show any change in presence of NB. The lowest value is around −1.1 kJ/mol. On the other hand, the minimum PMF value in the presence of OCT increases from −4.2 kJ/mol to −0.4 kJ/mol with an increase of PS length from 0PS to 3PS. Overall, it is observed from the PMF analysis that the solubility is higher in octanol compared to NB for both Gd^{3+}-DCHCE and UO_2^{2+}-DCHCE. Increase in the PS length on the DCHCE show minimal effect in octanol and no effect in NB.

Table 1
Coordination numbers for O_C–O_{NB}, O_C–N_{NB}, O_C–O_{OCT}, and O_C–H_{OCT}, pairs. The standard deviation values are within (±5–6%).

Pair	Gd^{3+}-DCHCE				UO_2^{2+}-DCHCE			
	0PS	1PS	2PS	3PS	0PS	1PS	2PS	3PS
O_C–O_{NB}	4.4	4.4	4.3	5.4	3.2	3.3	3.4	3.4
O_C–N_{NB}	4.4	4.2	4.4	5.0	6.1	6.0	6.2	6.2
O_C–O_{OCT}	3.0	2.6	2.5	3.0	1.1	1.1	1.2	0.9
O_C–H_{OCT}	1.0	0.9	0.9	0.9	0.8	0.7	0.7	0.7

3.3. Gd^{3+}-DCHCE and UO^{2+}-DCHCE ion binding structure

Fig. 6. presents the RDF between the Gd^{3+} and O_C of DCHCE. The first peak positions are located at ~0.24 nm for Gd^{3+} –O_C and ~0.23 nm for UO^{2+}–O_C in both NB and OCT. The peak position does not change with the increase in PS length from 0PS to 3PS. The observed peak position is similar to the RDF of Gd^{3+} –O_C, and UO_2^{2+}–O_C in DBCE [31,32]. The results obtained are in good agreement with the previous simulations study of Kim et al. [31] on the Gd^{3+} — crown-ether complex in the different organic solvents, where ~0.26 nm is observed for the first peak location of Gd^{3+} - O_C RDF. Similarly, the peak location of UO_2^{2+}-O_C is reported as 0.22 nm by a previous simulation study [32]. From all the results it is evident that the tight binding of Gd^{3+} and UO_2^{2+} seen in the NB, with the increase in PS length. The binding of these ions on to the DCHCE becomes slightly unfavorable with the increase in PS length in OCT as peak intensity shows a slight decrease with the increase in PS length.

3.4. Binding free-energy

Figs. 7 and 8 present the free-energy difference $\langle \partial U/\partial \lambda \rangle$ as a function of coupling parameter (λ). The binding free energy is estimated by growing the Gd^{3+} and UO_2^{2+} in the cavity of DCHCE as given by

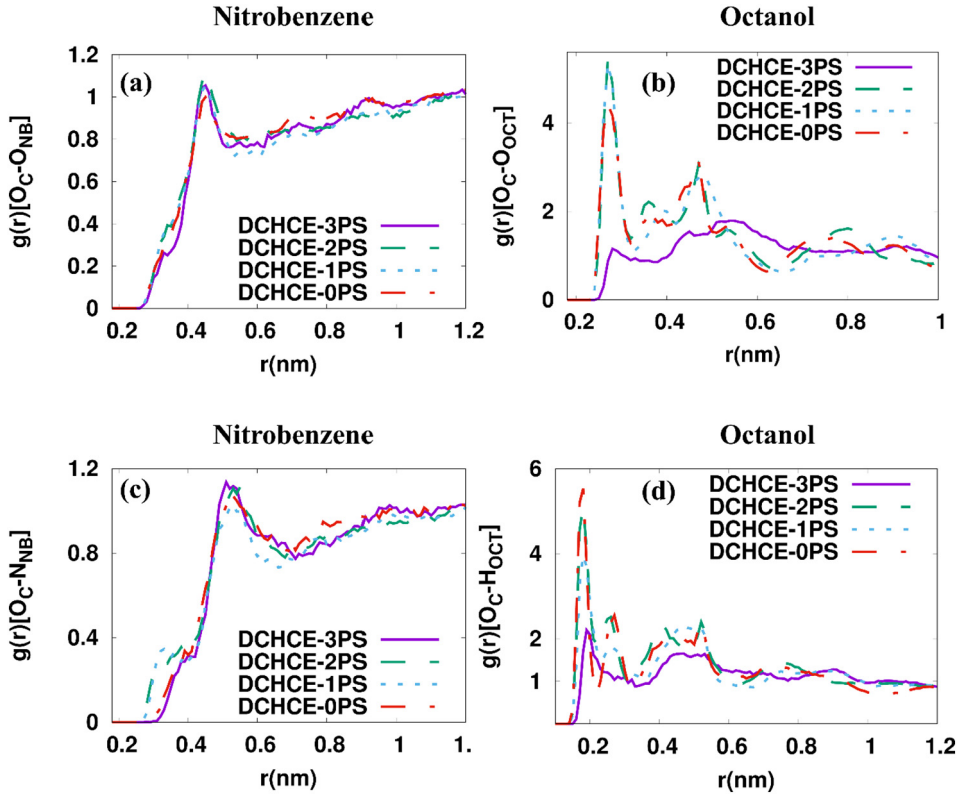

Fig. 4. RDF plot of (a) O_C-O_{NB}, (b) O_C-O_{OCT}, (c) O_C-N_{NB} and (d) O_C-H_{OCT} for UO_2^{2+}-DCHCE.

Eqs. (2) and (3) by using two-stage thermodynamic integration in the presence of organic solvents NB and OCT. It is evident from the figures that the electrostatic interaction plays a significant role in the evaluation of binding free energy for both the Gd^{3+} and UO_2^{2+} metal ions. The potential energy gradient $\langle \partial U/\partial \lambda \rangle$ for electrostatic coupling becomes more negative with increasing λ value from 0 to 1 in both the solvents NB and OCT.

This behavior is in good agreement with a previous study of Gd^{3+} and UO^{2+} binding in the cavity of DBCE [16]. The $\langle \partial U/\partial \lambda \rangle$ for electrostatic coupling do not show significant change, with increasing λ, for an increase in PS grafting length from 0PS to 3PS in NB and OCT for both Gd^{3+} and UO_2^{2+}. The $\langle \partial U/\partial \lambda \rangle$ value for van der Waals coupling shows favorable nature with an increase in PS grafting length in the range of $0.6 < \lambda < 1$ for both the metal ions Gd^{3+} and UO_2^{2+} in NB. In OCT $\langle \partial U/\partial \lambda \rangle$ for van der Waals coupling becomes unfavorable with an increase in PS length with increasing λ value from 0 to 1. The unfavorable binding for both Gd^{3+} and UO_2^{2+} in OCT can be seen in the range of $0.2 < \lambda < 0.6$ with an increase in PS length from 0PS to 3PS. This behavior is attributed to the unfavorable contribution of the cyclohexane ring on the DCHCE in OCT as observed in the increasing $\langle \partial U/\partial \lambda \rangle$ value with an increase in PS length.

Fig. 9 presents the ΔG_{Bind} as a function of PS length. The ΔG_{Bind} of Gd^{3+} becomes more favorable in going from 0PS to 1PS, but remains constant with further increase in PS length in the presence of NB. ΔG_{Bind} of Gd^{3+} becomes unfavorable with an increase in PS length from 0 PS to 3 PS in OCT. A similar kind of behavior is seen in ΔG_{Bind} for UO_2^{2+} in NB with an increase in PS length from 0 PS to 3 PS. An important observation that we have found in this work is that OCT becomes unfavorable for both metal ions as the length of PS chain is increased, which is unlike the case of our previous study [16], where the free energy of binding became favorable with increase in PS length from 0PS to 3 PS in the presence of both NB and OCT.

The presence of cyclohexane ring on the crown-ether (18C6) displays an unfavorable contribution towards the OCT as an extractant

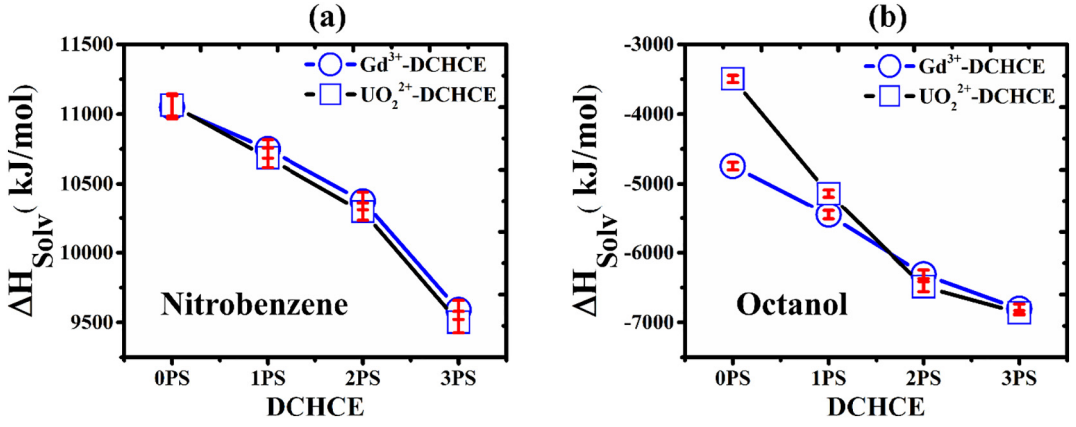

Fig. 5. Solvation enthalpy (ΔH_{solv}) of Gd^{3+}-DCHCE and UO_2^{2+}-DCHCE in two different solvents (a) NB and (b) OCT.

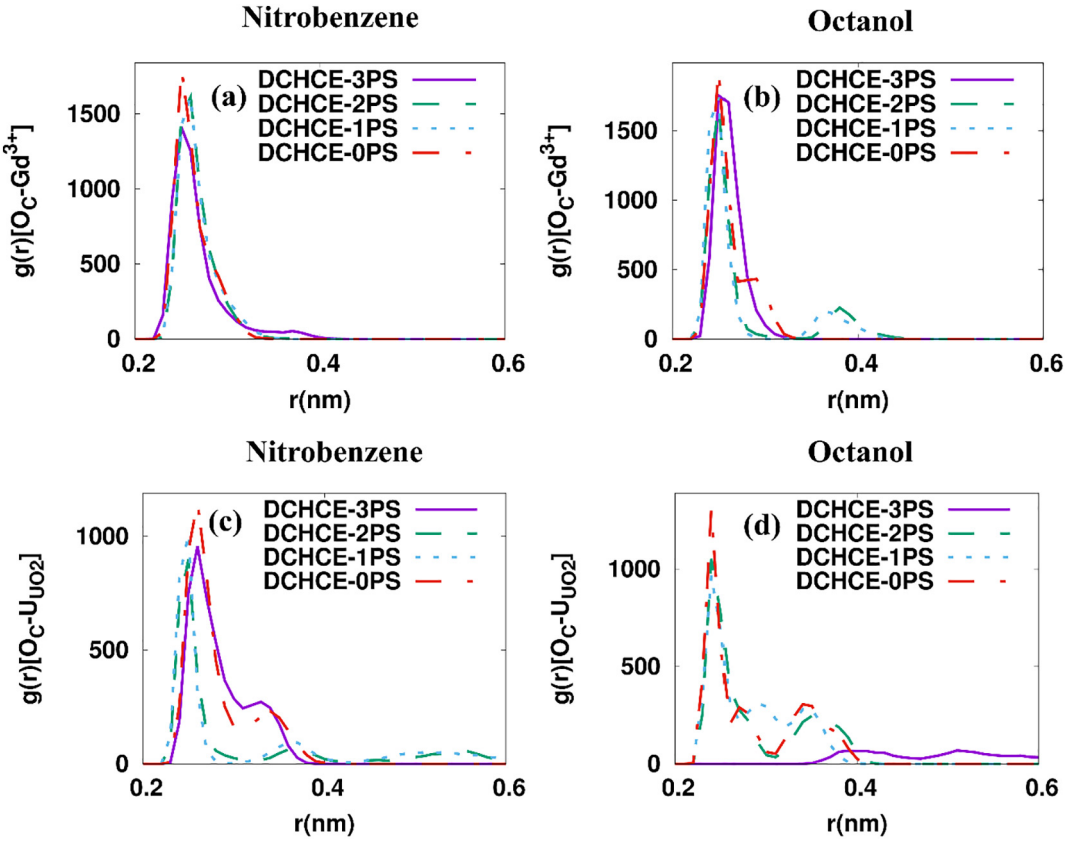

Fig. 6. RDF plot of O_C-Gd^{3+} for (a) NB (b) OCT and O_C-U_{UO2} for (c) NB (d) OCT.

for the extraction of these heavy metal ions. The dispersive interactions originating between cyclohexane and OCT are responsible for these adverse interactions upon increase in PS length. This behavior is visible in the curves presented in Figs. 3(d) and 4(d), where the $\langle \partial U/\partial \lambda \rangle$ show unfavorable values for the binding behavior in the range of $0.2 < \lambda < 0.6$ with an increase in PS length from 0 PS to 3 PS. It also observed that ΔG_{Bind} of (Gd^{3+}) is two-fold higher than that of ΔG_{Bind} of (UO_2^{2+}) in both the solvents over the entire range of PS varying from 0PS to

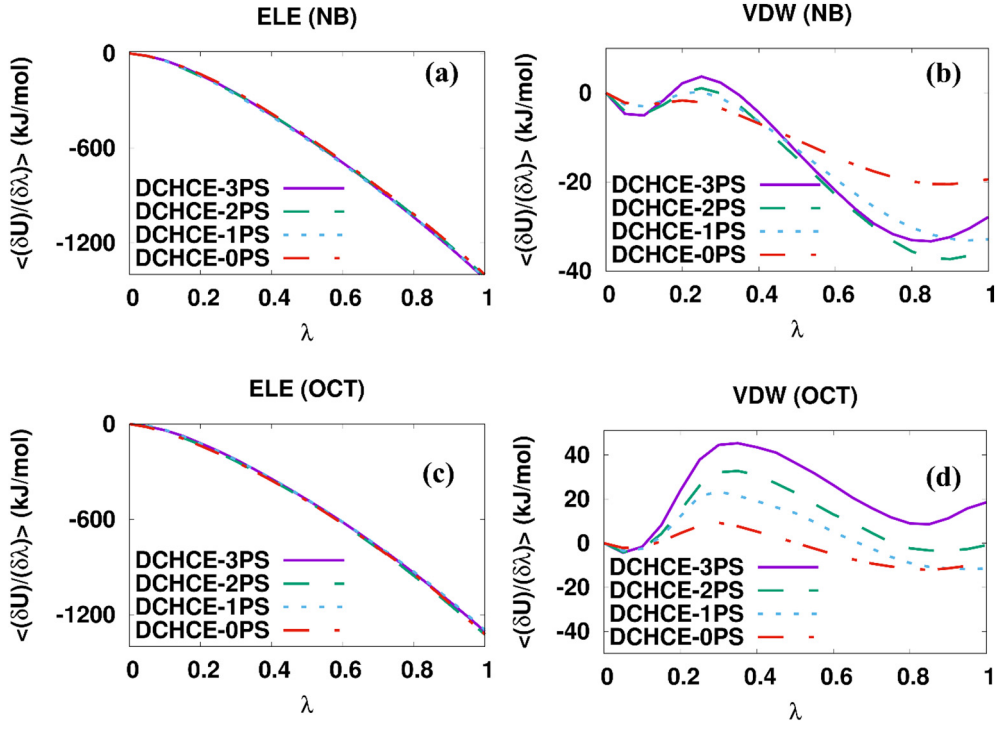

Fig. 7. The free energy difference $\langle \partial U/\partial \lambda \rangle$ for Gd^{3+} ion with an increase in polystyrene length in the presence of NB ((a) and (b)) and OCT ((c) and (d)).

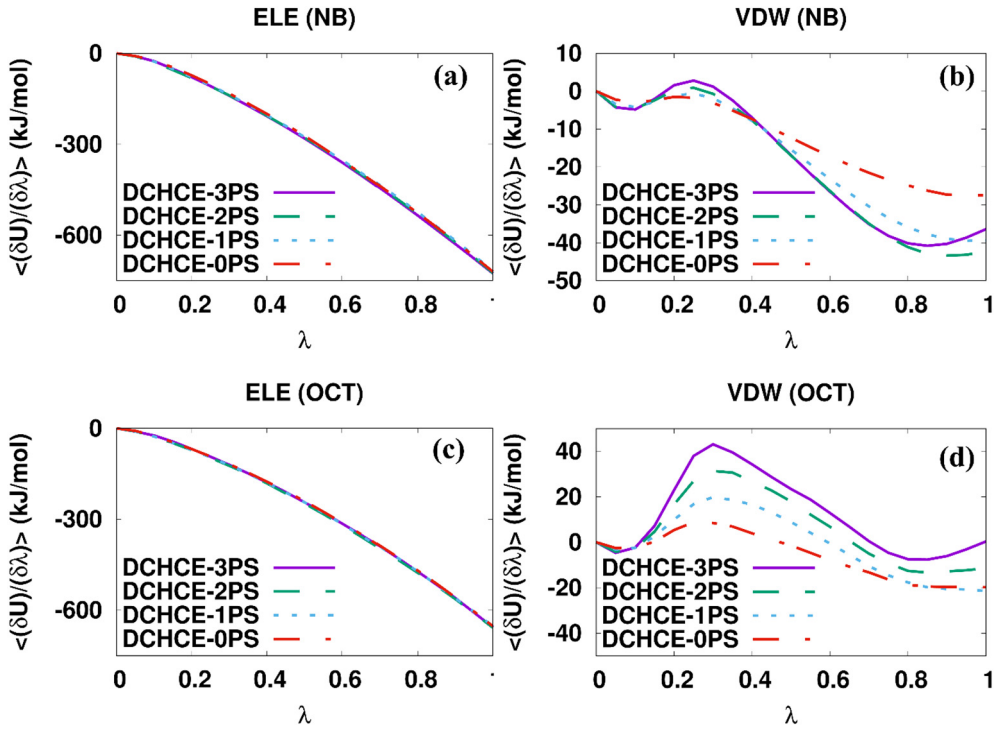

Fig. 8. The free energy difference $\langle \partial U/\partial \lambda \rangle$ for UO_2^{2+} on with an increase in polystyrene length in the presence of NB ((a) and (b)) and OCT ((c) and (d)).

3PS. There are no direct experimental results till date for a quantitative or qualitative comparison of ΔG_{Bind} of Gd^{3+} and UO_2^{2+}, as a function of PS length, on the DCHCE in NB and OCT solvents.

However, a gas phase study [33] predicted the binding energy of Gd^{3+} on EDTA ligand as −4424.7 kJ/mol. In the current work, we have obtained lower higher values of ΔG_{Bind} values for Gd^{3+} and UO_2^{2+} in NB and OCT solvents because of the realistic explicit description of solvent molecules. Fig. 5(a) shows the favorable binding free energy of these metal ions in the presence of NB, as seen from ΔH_{solv} calculation. A similar behavior is seen on the solvation structure of Gd^{3+} and UO_2^{2+} complexed DCHCE, displaying an unfavorable contribution with the increase in PS length on DCHCE in OCT. Thus, observed structural characteristics are in accordance with the binding free energy calculations as discussed above and draw a similar conclusion on OCT viz., OCT provides unfavorable environment for the Gd^{3+} and UO_2^{2+} binding on to the DCHCE.

3.5. Transfer free-energy

The transfer free-energy ($\Delta G_{Transfer}$) of Gd^{3+} and UO_2^{2+} from an aqueous phase to an organic phase is calculated using Eq. (3). To estimate the $\Delta G_{Transfer}$ first, we evaluated the hydration free-energy of Gd^{3+} and UO^{2+} in an aqueous solution. The hydration free energy calculated are −2897.6 ± 3.6 kJ/mol for Gd^{3+} and −1274.6 ± 1.9 kJ/mol for UO_2^{2+}, which are in close agreement with the previous reported theoretical results [34,35]. The calculated hydration free energy ($\Delta G_{Hydration}$) (in 3 M HNO_3) of Gd^{3+} is −2934 ± 2.05 kJ/mol, and for UO_2^{2+} it is −1310 ± 2.28 kJ/mol. It is observed that addition of HNO_3 increases the $\Delta G_{Hydration}$ values, as seen for pure aqueous solution for which $\Delta G_{Hydration}$ increases by ~1.3%. Fig. S3 of the supplementary data file presents the effect of the acidic medium on the transfer free energy $\Delta G_{Transfer}$. The reported values of the hydration of free energy for Gd^{3+} is −3429.2 kJ/mol [34], and

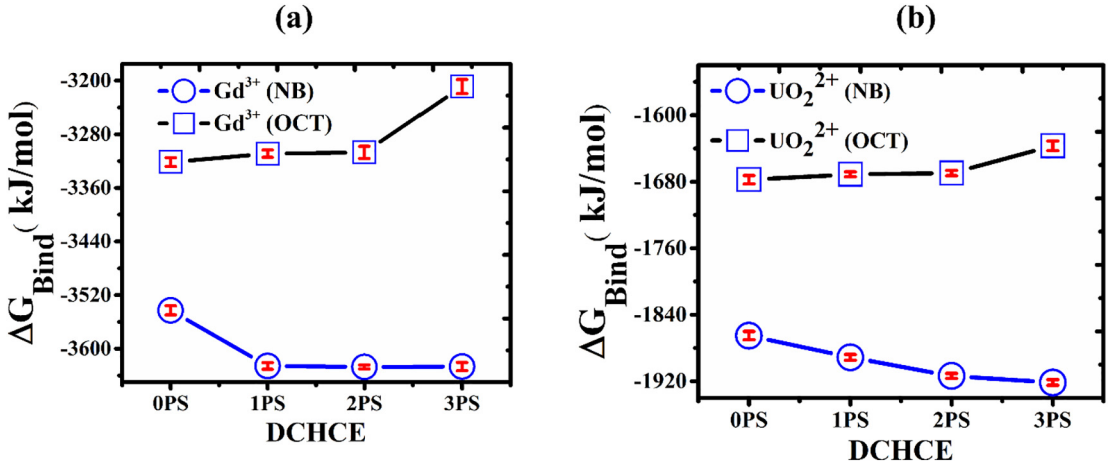

Fig. 9. Binding free energy (ΔG_{Bind}) as function of PS length (a) Gd^{3+} and (b) UO_2^{2+}.

−1267.7 kJ/mol for UO_2^{2+} [35]. We obtained slightly lower values of hydration free energy for Gd^{3+} than the reported values [34]. This is mainly due to the different treatment of the solvent. In the earlier work of van Veggel et al. [34], water is considered as a dielectric medium. In this current work we have considered the real solvent with explicit description.

Fig. 10 presents $\Delta G_{Transfer}$ of the Gd^{3+} and UO_2^{2+} from an aqueous phase to an organic phase. It is clear from the figure that the $\Delta G_{Transfer}$ for the Gd^{3+} and UO_2^{2+} becomes favorable in NB, as an extractant, while it becomes unfavorable if OCT is used as an extractant with an increase in PS from 0 PS to 3 PS. This observation is in accordance with the binding free energy calculation as discussed above. The acidic medium also has an effect on $\Delta G_{Transfer}$ for the both Gd^{3+} and UO_2^{2+} over the grafting length of 0PS to 3PS. The $\Delta G_{Transfer}$ show a ~6% increase with nitrobenzene and ~9% increase with octanol, for both Gd^{3+} and UO_2^{2+} in 3 M HNO_3. The unfavorable van der Waals interactions between OCT and cyclohexane ring on the DCHCE is the key reason behind this kind of behavior. In a previous work [16] OCT was found favorable for the transfer of Gd^{3+} and UO_2^{2+} from the aqueous phase to octanol phase, where we observe an attractive contribution between the benzene ring on the DBCE with the aliphatic group of octanol. Thus, a small structural change in the extractant can cause significant effect on the transfer free-energy. This is also observed in a theoretical study by Kim [36], where it is shown that a small structural change in extractant leads to a significant influence on the Sr^{2+} transfer. From our present work and previous literatures [16,36,37], it is evident that the small change in the chemical structure can lead to significant change in its thermodynamic behavior. The observed order of $\Delta G_{Transfer}$ for both Gd^{3+} and UO_2^{2+} in NB is 3PS > 2PS > 1PS > 0PS, whereas an opposite behavior is seen in OCT as 0PS > 1PS > 2PS > 3PS.

3.6. Partition coefficient

The partition of solutes or ions from the one phase to another phase is traditionally better understood by calculating the partition coefficient log P. Fig. 11 presents the log P values calculated using Eq. (4) as a function of PS length. It is observed that log P value increases with the increase in PS length in NB while its value decreases in OCT. The values of log P increase as a function of PS length from 112 to 126 for Gd^{3+} and 102 to 112 for UO_2^{2+} in NB. The opposite behavior is seen in OCT as log P values show a decrease from 73 to 54 for Gd^{3+} and 70 to 63 for UO_2^{2+} with the increase in PS length from 0PS to 3PS. The effect of the acidic medium on the partition coefficient log P is presented in Fig. S4 in the supplementary data file. In the presence of acidic medium with increase in PS length the log P values show increase from 106 to 120 for Gd^{3+} and 97 to 106 for UO_2^{2+} in NB. On the other hand, the log P values show a decrease from 67 to 47 for Gd^{3+} and 64 to 57 for UO_2^{2+} in OCT. The log P value show a ~6% decrease with NB and ~ 9% decrease

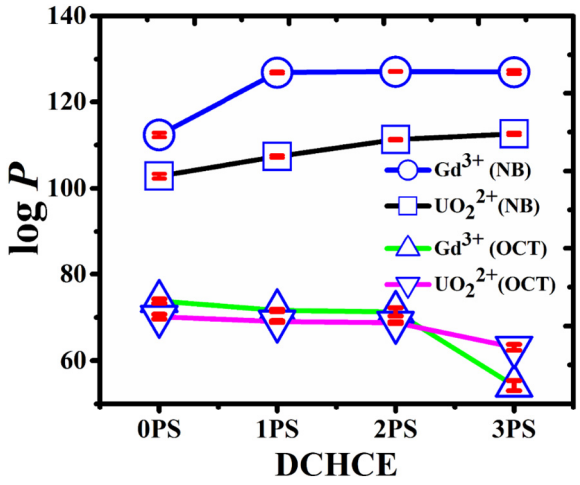

Fig. 11. Partition coefficient (log P) of Gd^{3+} and UO_2^{2+} as function of PS length.

with octanol for both Gd^{3+} and UO_2^{2+} in 3 M HNO_3 when compared to pure aqueous solution (without acidic medium). These observations are in accordance with results of ΔG_{Bind} and $\Delta G_{Transfer}$. In an earlier work, five-fold increase in log P values for both Gd^{3+} and UO_2^{2+} was reported in the case of DBCE in NB and OCT [16].

The changes in the log P values are minimal due to the effect of chain length, which is attributed to small structural difference on crown ether. Nevertheless, the PS effect on DCHCE is not that noteworthy when compared to DBCE for the partitioning of Gd^{3+} and UO_2^{2+} [16]. There are no available data for the quantitative comparison of log P values for Gd^{3+} and UO_2^{2+}. However, there are other ions which are well studied. For examples, an experimental study by Soto et al. [37] on Cd^{2+}, Ni^{2+} and Pb^{2+} ion adsorption on oxidized starches reported partition coefficient values of 95 to 135 for Cd^{2+}, 99 to 207 for Ni^{2+} and 58 to 280 for Pb^{2+} with an increase in oxidation. A simulation study by Kim et al. [36] has shown lower values of partition coefficient for Ba^{2+} in the range of 1–23 in carbon tetrachloride (CCL_4) and propane (C_3H_8). In the current work, the higher values of partition coefficient is an indication of enhanced partitioning of Gd^{3+} and UO_2^{2+} in NB and OCT. In the earlier work (Ref 16) the partition coefficient (log P) values, with di benzo crown ether (DBCE), varies as 88–222 for Gd^{3+} and 79–200 for UO_2^{2+} over the grafting length of 0PS to 3 PS in both solvents, NB and octanol. In the current work, the log P values varies as 54–126 for Gd^{3+} and 63–112 for UO^{2+} over the grafting length of 0PS to 3PS with both solvents NB and OCT. Based on the values of log P in the earlier work (Ref 16), and from the current work, it is observed that DCHCE exhibits a lower extracting capabilities compared to that of DBCE. It is evident that the small chemical structural change on the crown ether (i.e., benzene ring (DBCE) and cyclohexane ring (DCHCE) on crown

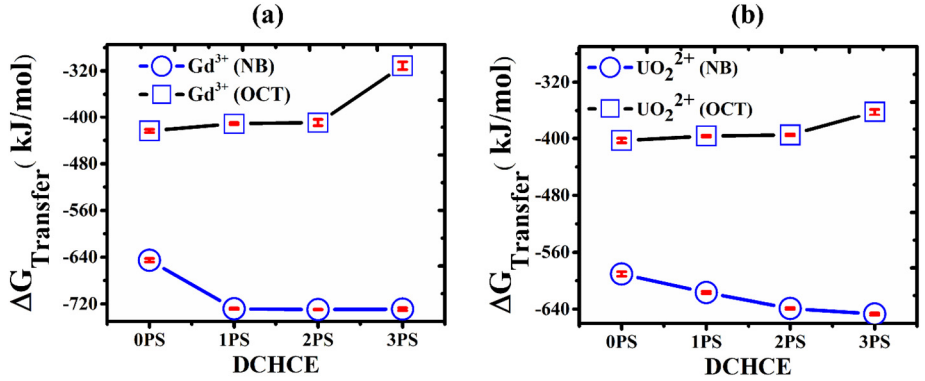

Fig. 10. Transfer free energy ($\Delta G_{Transfer}$) as function of PS length (a) Gd^{3+} and (b) UO_2^{2+}.

ether) can lead to significant influence on the metal ion binding (adsorption) and liquid-liquid extraction behavior.

4. Conclusions

The solvation structure and ΔH_{solv} of Gd^{3+}-DCHCE and UO_2^{2+}-DCHCE become favorable in NB and unfavorable in OCT with an increase in PS length. The RDF peak position located at ~0.24 nm for Gd^{3+}-O_C and ~0.23 nm for UO^{2+}-O_C in both NB and OCT which do change with the increase in PS length from 0PS to 3PS. The ΔG_{Bind} of Gd^{3+} and UO_2^2 becomes favorable in NB and unfavorable in OCT with the increase in PS length from 0PS to 3 PS. In OCT the unfavorable binding interaction for Gd^{3+} and UO_2^{2+} seen in the range of $0.2 < \lambda < 0.6$ with an increase in PS length from 0PS to 3PS. It is concluded that the dispersive interactions arising between cyclohexane and OCT would be responsible for this unfavorable binding interaction for Gd^{3+} and UO_2^{2+} on to the DCHCE in OCT with an increase in PS length. $\Delta G_{Transfer}$ for the Gd^{3+} and UO_2^{2+} becomes favorable using NB as an extractant with an increase of PS from 0PS to 3PS. However, it shows unfavorable nature when OCT is used as an extractant. These observations are in akin to the binding free energy calculations. The observed $\Delta G_{Transfer}$ of both Gd^{3+} and UO_2^{2+} is favorable in NB and follows the order with changing PS grafting length as 3PS > 2PS > 1PS > 0PS, while an opposite behavior 0PS > 1PS > 2PS > 3PS is seen in OCT. Similar behavior is observed for log P values in both solvents with increasing PS length. The log P values show an increase from 112 to 126 for Gd^{3+} and 102 to 112 for UO_2^{2+} in NB. In OCT, the log P values decrease from 73 to 54 and 70 to 63 respectively for Gd^{3+} and UO_2^{2+}. The presence of acidic medium show a 6–9% increase in $\Delta G_{Transfer}$ and 6–9% decrease in log P for the both Gd^{3+} and UO_2^{2+} over the grafting length of 0PS to 3PS. These observations are in accordance with results of ΔG_{Bind}. From our results, we conclude that NB is favorable extractant for heavy metal ions such as Gd^{3+} and UO_2^{2+} as compared to OCT in aqueous solution. It is also deduced that grafting the DCHCE becomes favorable in NB.

Acknowledgment

This work is supported by The Board of Research in Nuclear Sciences (BRNS), Department of Atomic Energy (DAE), and Government of India, sanctioned no: 36(1)/14/02/2015-BRNS/100. We are grateful to HPC, IIT Kanpur for the computational support. PKS gratefully acknowledges Science and Engineering Research Board (SERB), Department of Science and Technology (DST), Government of India, for the National Post-Doctoral Fellowship (PDF/2017/000121).

Appendix A. Supplementary data

Supporting Information is available: partial atomic charges and force-field parameters for Gd^{3+}-DCHCE and UO_2^{2+}-DCHCE with an increase in PS chain length. Supplementary data to this article can be found online at https://doi.org/10.1016/j.molliq.2018.08.133.

References

[1] M. Lemaire, A. Guy, R. Chomel, J. Foos, Dicyclohexano-18-crown-6 ether: a new selective extractant for nuclear fuel reprocessing, J. Chem. Soc. Chem. Commun. 17 (1991) 1152–1154.
[2] G. Ranghino, S. Romans, J.M. Lehn, G. Wipff, Monte Carlo study of the conformation-dependent hydration of the 18-crown-6 macrocycle, J. Am. Chem. Soc. 107 (1985) 7873–7877.
[3] G. Ye, F. Bai, J. Wei, J. Wang, J. Chen, Novel polysiloxane resin functionalized with dicyclohexano-18-crown-6 (DCH18C6): synthesis, characterization and extraction of Sr (II) in high acidity HNO_3 medium, J. Hazard. Mater. 225 (2012) 8–14.
[4] G.H. Rounaghi, S. Heydari, A thermodynamic study of complex formation between dicyclohexyl-18-crown-6 (DCH18C6) and La^{3+}, UO_2^{2+}, Ag^+, and NH^{4+} cations in acetonitrile-tetrahydrofuran binary media using conductometric method, Russ. J. Coord. Chem. 34 (2008) 836–841.
[5] J.N. Mathur, P.K. Khopkar, Use of crown ethers as synergists in the solvent extraction of trivalent actinides and lanthanides by 1-phenyl-3-methyl-4 trifluoroacetyl pyrazolone-5, Solvent Extr. Ion Exch. 6 (1988) 111–124.
[6] S.V. Demin, V.I. Zhilov, A.Y. Tsivadze, V.V. Yakshin, O.N. Vilkova, N.A. Tsarenko, Extraction of rare-earth elements by alkylated dibenzo-18-crown-6 and dicyclohexano-18-crown-6 from acid solutions, Russ. J. Inorg. Chem. 51 (2006) 1678–1681.
[7] G.H. Rounaghi, S. Heydari, Study of complex formation between dicyclohexyl-18-crown-6 with La^{3+}, UO_2^{2+}, Ag^+ and NH_4^+ cations in acetonitrile-nitromethane binary mixtures, Asian J. Chem. 20 (2008) 535.
[8] E. Karkhaneei, M.H. Zebarjadian, M. Shamsipur, Complexation of Ba^{2+}, Pb^{2+}, Cd^{2+}, and UO_2^{2+} ions with 18-crown-6 and dicyclohexyl-18-crown-6 in nitromethane and acetonitrile solutions by a competitive NMR technique using the 7Li nucleus as a probe, J. Solut. Chem. 30 (2001) 323–333.
[9] T. Kuokkanen, Effect of ring size on the complexation and decomposition of benzenediazonium ion in the presence of crown ethers in 1, 2-dichloroethane and the gas phase, J. Phys. Org. Chem. 10 (1997) 67–75.
[10] C.J. Pedersen, Cyclic polyethers and their complexes with metal salts, J. Am. Chem. Soc. 89 (1967) 7017–7036.
[11] E.T.H. Leuwerink, S. Harkema, W.J. Briels, D. Feil, Molecular dynamics of 18-crown-6 complexes with alkali–metal cations and urea: prediction of their conformations and comparison with data from the Cambridge structural database, J. Comput. Chem. 14 (1993) 899–906.
[12] P. Sahu, S.M. Ali, J.K. Singh, Structural and dynamical properties of Li^+-dibenzo-18-crown-6 (DB18C6) complex in pure solvents and at the aqueous-organic interface, J. Mol. Model. 20 (2014) 2413.
[13] S. De, A. Boda, S.M. Ali, Preferential interaction of charged alkali metal ions (guest) within a narrow cavity of cyclic crown ethers (neutral host): a quantum chemical investigation, J. Mol. Struct. (THEOCHEM) 941 (2010) 90–101.
[14] A. Boda, S. De, S.M. Ali, S. Tulishetti, S. Khan, J.K. Singh, From microhydration to bulk hydration of Sr^{2+} metal ion: DFT, MP2 and molecular dynamics study, J. Mol. Liq. 172 (2012) 110–118.
[15] A. Boda, A.S. Deb, S.M. Ali, K.T. Shenoy, S. Mohan, Molecular engineering of functionalized crown ether resins for the isotopic enrichment of gadolinium: from computer to column chromatography, Mol. Sys. Des. Eng. 2 (2017) 640–652.
[16] P. Sappidi, S. Namsani, S.M. Ali, J.K. Singh, Extraction of Gd^{3+} and UO_2^{2+} ions using polystyrene grafted dibenzo crown ether (DB18C6) with octanol and nitrobenzene: a molecular dynamics study, J. Phys. Chem. B 122 (2018) 1334–1344.
[17] R. Sinta, P.S. Rose, J. Smid, Formation constants of complexes between crown ethers and alkali picrates in apolar solvents. Application of crown ether network polymers, J. Am. Chem. Soc. 105 (1983) 4337–4343.
[18] A. Bey, O. Dreyer, V. Abetz, Thermodynamic analysis of alkali metal complex formation of polymer-bonded crown ether, Phys. Chem. Chem. Phys. 19 (2017) 15924–15932.
[19] Accelrys Software Inc, Materials Studio Modeling Environment, Release 5.0, Accelrys Software Inc., San Diego, USA, 2007.
[20] M.J. Frisch, G.W. Trucks, H.B. Schlegel, G.E. Scuseria, M.A. Robb, J.R. Cheeseman, H. Nakatsuji, et al., Gaussian 09 Revision D. 01, 2009.
[21] C. Lee, W. Yang, R.G. Parr, Development of the Colle-Salvetti correlation-energy formula into a functional of the electron density, Phys. Rev. B 37 (1988) 785.
[22] L.E. Chirlian, M.M. Francl, Atomic charges derived from electrostatic potentials: a detailed study, J. Comput. Chem. 8 (1987) 894–905.
[23] W.L. Jorgensen, D.S. Maxwell, J. Tirado-Rives, Development and testing of the OPLS all-atom force field on conformational energetics and properties of organic liquids, J. Am. Chem. Soc. 118 (1996) 11225–11236.
[26] T. Darden, D. York, L. Pedersen, Particle mesh Ewald: an N·log (N) method for Ewald sums in large systems, J. Chem. Phys. 98 (1993) 10089–10092.
[27] B. Hess, H. Bekker, H.J. Berendsen, J.G. Fraaije, LINCS: a linear constraint solver for molecular simulations, J. Comput. Chem. 18 (1997) 1463–1472.
[28] S. Pronk, S. Páll, R. Schulz, P. Larsson, P. Bjelkmar, R. Apostolov, B. Hess, et al., GROMACS 4.5: a high-throughput and highly parallel open source molecular simulation toolkit, Bioinformatics 29 (2013) 845–854.
[29] C.C. Bannan, G. Calabró, D.Y. Kyu, D.L. Mobley, Calculating partition coefficients of small molecules in octanol/water and cyclohexane/water, J. Chem. Theory Comput. 12 (2016) 4015–4024.
[30] N.M. Garrido, A.J. Queimada, M. Jorge, E.A. Macedo, I.G. Economou, 1-Octanol/water partition coefficients of n-alkanes from molecular simulations of absolute solvation free energies, J. Chem. Theory Comput. 5 (2009) 2436–2446.
[31] H.S. Kim, K.W. Chi, Monte Carlo simulation study for QSPR of solvent effect on the selectivity of 18-crown-6 between Gd^{3+} and Yb^{3+} ions, J. Mol. Struct. (THEOCHEM) 722 (2005) 1–7.
[32] P. Guilbaud, G. Wipff, Selective complexation of UO_2^{2+} by the calix [6] arene 6— anion: structure and hydration studied by molecular dynamics simulations, J. Incl. Phenom. Mol. Recognit. Chem. 16 (1993) 169–188.
[33] A. Boda, S.K. Arora, A.K. Singha Deb, M. Jha, S.M. Ali, K.T. Shenoy, Molecular modeling guided isotope separation of gadolinium with strong cation exchange resin using displacement chromatography, Sep. Sci. Technol. (2016) 1–8.
[34] F.C. van Veggel, D.N. Reinhoudt, New, accurate Lennard-Jones parameters for trivalent lanthanide ions, tested on [18] crown–6, Chem. Eur. J. 5 (1999) 90–95.
[35] P. Guilbaud, G. Wipff, Hydration of uranyl (UO_2^{2+}) cation and its nitrate ion and 18-crown-6 adducts studied by molecular dynamics simulations, J. Phys. Chem. 97 (1993) 5685–5692.
[36] H.S. Kim, A Monte Carlo simulation study of solvent effect on Ba^{2+} to Sr^{2+} ion mutation, Phys. Chem. Chem. Phys. 2 (2000) 2919–2923.
[37] D. Soto, J. Urdaneta, K. Pernía, O. León, A. Muñoz-Bonilla, M. Fernández-García, Heavy metal (Cd^{2+}, Ni^{2+}, Pb^{2+}, and Ni^{2+}) adsorption in aqueous solutions by oxidized starches, Polym. Adv. Technol. 26 (2015) 147–152.